HOKKAIDO UNIVERSITY

Title	JAK/STAT guarantees robust neural stem cell differentiation by shutting off biological noise
Author(s)	Tanaka, Yoshitaro; Yasugi, Tetsuo; Nagayama, Masaharu et al.
Citation	Scientific reports, 8, 12484 https://doi.org/10.1038/s41598-018-30929-1
Issue Date	2018-08-20
Doc URL	https://hdl.handle.net/2115/71998
Rights(URL)	https://creativecommons.org/licenses/by/4.0/
Type	journal article
File Information	s41598-018-30929-1.pdf

Hokkaido University Collection of Scholarly and Academic Papers : HUSCAP

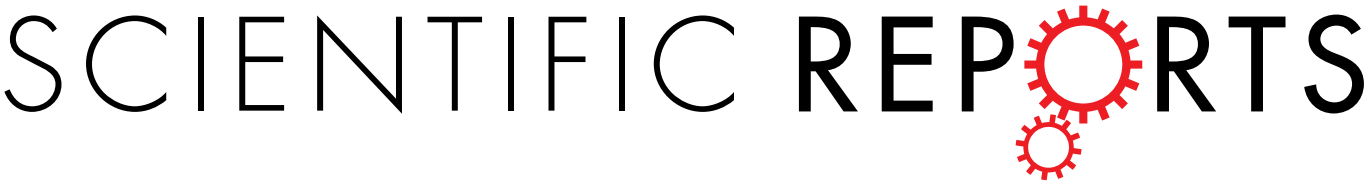

OPEN

JAK/STAT guarantees robust neural stem cell differentiation by shutting off biological noise

Received: 3 October 2017
Accepted: 8 August 2018
Published online: 20 August 2018

Yoshitaro Tanaka[1,5], Tetsuo Yasugi[2], Masaharu Nagayama[3], Makoto Sato[2,4] & Shin-Ichiro Ei[1]

Organismal development is precisely regulated by a sequence of gene functions even in the presence of biological noise. However, it is difficult to evaluate the effect of noise *in vivo*, and the mechanisms by which noise is filtered during development are largely unknown. To identify the noise-canceling mechanism, we used the fly visual system, in which the timing of differentiation of neural stem cells is spatio-temporally ordered. Our mathematical model predicts that JAK/STAT signaling contributes to noise canceling to guarantee the robust progression of the differentiation wave *in silico*. We further demonstrate that the suppression of JAK/STAT signaling causes stochastic and ectopic neural stem cell differentiation *in vivo*, suggesting an evolutionarily conserved function of JAK/STAT to regulate the robustness of stem cell differentiation.

During development, stochastic noise arises to varying degrees. Stochastic gene expression and fluctuation of proteins occur intrinsically, caused by the probabilistic collisions between molecules. In addition, cell divisions and external forces from the environment often affect cell positioning and cell fate decisions. Any individual multicellular organism can robustly develop even under these intrinsic and extrinsic sources of noise. Therefore, noise resistance is one of the essential properties of the developing multicellular organisms[1]. For robust gene expression in a cell, negative feedback is one of the major ways to reduce the effects of stochastic noise[2,3]. Similarly, the ratio of transcription frequency to translation frequency attenuates intrinsic noise[4]. It has been reported that intercellular Notch signaling plays the crucial role to minimize the noise for consistent coherent oscillation during somite segmentation[5]. However, the specific mechanisms of the noise resistance in developing multicellular systems have rarely been identified.

Mathematical modeling is a useful tool for estimating the effects of stochastic noises and fluctuations in biological systems. For unicellular organisms, stochastic models can be used to control and regulate the stochastic gene expression levels and the fluctuation of protein expression[2,6,7]. These models are usually described as simple ordinary differential equations (ODEs) by assuming that the mutual interaction among networks is linear. For multicellular organisms, it is necessary to construct the mathematical model based on partial differential equations (PDEs) and/or the ODEs with intercellular interactions because intercellular signaling plays significant roles in the development of multicellular organisms. By varying the values of the parameters in the mathematical models, we can observe the behaviors of the solutions corresponding to the biological phenomena, and we can easily add small amounts of noise to the specified regions in the numerical simulations. Moreover, if we use simple biological models such as the fruit fly, we can adapt the parameters of the mathematical models to the real genes in the network systems, and we can freely manipulate them in the numerical simulations. Thus, by changing the parameters in the numerical simulations in the presence of noise and observing the numerical results of the mathematical model, we can directly identify the gene network relating to the robustness against the biological noises.

To theoretically and experimentally investigate how multicellular organisms cope with biological noise, the developing fly visual system provides an excellent model. The wave of differentiation called the "proneural wave"

[1]Department of Mathematics, Faculty of Science, Hokkaido University, Kita 10, Nishi 8, Kita-Ku, Sapporo, Hokkaido, 060-0810, Japan. [2]Mathematical Neuroscience Unit, Institute for Frontier Science Initiative, Kanazawa University, 13-1 Takaramachi, Kanazawa-shi, Ishikawa, 920-8640, Japan. [3]Research Institute for Electronic Science, Hokkaido University, Kita 12, Nishi 7, Kita-ku, Sapporo, Hokkaido, 060-0812, Japan. [4]Laboratory of Developmental Neurobiology, Graduate School of Medical Sciences, Kanazawa University, 13-1 Takaramachi, Kanazawa-shi, Ishikawa, 920-8640, Japan. [5]Present address: Department of Complex and Intelligent Systems, School of Systems Information Science, Future University Hakodate, 116-2 Kamedanakano-cho, Hakodate, Hokkaido, 041-8655, Japan. Yoshitaro Tanaka and Tetsuo Yasugi contributed equally. Correspondence and requests for materials should be addressed to M.S. (email: makotos@staff.kanazawa-u.ac.jp) or S.-I.E. (email: Eichiro@math.sci.hokudai.ac.jp)

sweeps across the surface of the brain during the third larval instar (Fig. 1A)[8,9]. During the progression of the proneural wave, neuroepithelial cells (NEs) sequentially differentiate into neuroblasts (NBs), neural stem-like cells. This progression starts at the medial edge of the NE sheet and extends toward the lateral edge. The differentiating cells start expressing Achaete-Scute Complex (AS-C) proneural proteins such as Scute, Lethal of Scute (L'sc), and Asense (Ase)[8]. Among them, L'sc is transiently expressed in cells at the transition interface between NEs and NBs and acts as a trigger for NB differentiation (Fig. 1A,F–H')[8]. During the progression of the proneural wave, several signaling pathways, including EGF, Notch, JAK/STAT, and Hippo, play pivotal roles[8–12]. The EGF and Notch signaling pathways are activated in the wavefront cells and regulate the progression of the wave positively and negatively, respectively (Fig. 1A,C)[9,12]. By combining mathematical modeling with genetic experiments, we have previously reported that Notch-mediated lateral inhibition is implemented within the progression of the proneural wave, though Notch activation does not show a salt and pepper pattern[13].

In this study, we show that our previous mathematical model lacks noise resistance. This raises a possibility that there is a noise-canceling mechanism during the progression of the proneural wave *in vivo*. To improve our previous model, we focus on the function of JAK/STAT signaling, which has been shown to negatively regulate the progression of the wave *in vivo*[8]. The modified version of the mathematical model cancels the effect of noise and shows the robust progression of the wave. We further demonstrate that suppression of the function of *Stat92E* shows ectopic and random NB differentiation *in vivo*. Our *in silico* and *in vivo* data indicate that JAK/STAT signaling plays a critical role in noise canceling during neural stem cell differentiation.

Results

Mild EGF noise induces ectopic neuroblast differentiation in the previous mathematical model. To understand the complex interplay among EGF, Notch, and AS-C during the propagation of the proneural wave, we have previously developed a mathematical model based on the molecular interactions identified through a series of genetic experiments (Fig. 1D,E)[13]. We have applied the diffusion model for EGF and the lateral inhibition mechanism for Notch and have represented the mutual interactions as follows:

$$(Model\ 1)\begin{cases} \dfrac{\partial E}{\partial t} = d_e\Delta E - k_e E + a_e A(A_0 - A), \\ \dfrac{dN_{i,j}}{dt} = -k_n N_{i,j} + d_t \sum\limits_{l,m\in\Lambda_{i,j}} D_{l,m} - d_c N_{i,j} D_{i,j}, \\ \dfrac{dD_{i,j}}{dt} = -k_d D_{i,j} + a_d A_{i,j}(A_0 - A_{i,j}), \\ \dfrac{dA_{i,j}}{dt} = e_a(A_0 - A_{i,j})\max\{E_{i,j} - N_{i,j}, 0\}. \end{cases} \quad (x, y) \in B,\ t > 0, \tag{1}$$

Here, E is a composite variable for the EGF ligand concentration and EGF signaling at position x and time t, $N_{i,j}$ and $D_{i,j}$ are variables for Notch signal activity and Dl expression in the ith and jth cells at time t, respectively, $A_{i,j}$ is a variable for the level of the differentiation of AS-C in the ith and jth cells at time t, and d_e, k_e, a_e, k_n, d_t, d_c, k_d, a_d, e_a are positive constants (see materials and methods for other definitions). This suggests that the combination of the reaction diffusion system of EGF and the lateral inhibition system of Notch accurately mimics *in vivo* situations in wild-type animals and mutants for EGF or Notch signaling components[13].

Although Model 1 reproduces experimental results for the progression of the proneural wave, it lacks the noise resistance. The addition of noise for EGF in the numerical simulation causes stochastic NB differentiation apart from the proneural wavefront (Fig. 2). The numerical results of Model 1 with the addition of a small amount perturbation of the EGF level away from the wavefront at the white arrow shows the propagation of spontaneous NB differentiation in the region distant from the wavefront. In contrast, the effect of artificial activation of EGF signaling ahead of the wavefront is very limited *in vivo*. Although ectopic NB differentiation is induced, it does not propagate to the surrounding undifferentiated region[12]. The difference between *in silico* and *in vivo* experiments suggests that there is a noise-canceling mechanism to ensure the robust progression of the differentiation wave *in vivo*.

JAK/STAT signaling suppresses the effect of noise during the progression of the proneural wave *in silico*. As a candidate mechanism for the noise canceling, we focused on the function of JAK/STAT signaling based on previous findings. First, Unpaired (Upd), a ligand for JAK/STAT signaling, is expressed in lateral NEs and forms a gradient of JAK/STAT signaling, which is higher laterally and lower medially (Fig. 1C, Fig. S1)[8]. Second, JAK/STAT signaling negatively regulates the progression of the proneural wave; therefore, suppression of JAK/STAT signaling results in faster progression of the proneural wave (Fig. 1B)[8]. Third, JAK/STAT signaling positively regulates the expression of a subset of Notch target genes, including *Enhancer of split mδ* (*E(spl) mδ*), *Enhancer of split m7* (*E(spl)m7*), and *Twin of m4* (*Tom*), in the fly brain[14]. We therefore improved Model 1 by incorporating the effect of JAK/STAT into the system. Based on previous findings, we added the following assumptions to construct the mathematical models with noise resistance:

(A.1) JAK/STAT activates the expression of a subset of Notch target genes that inhibit the expression of the AS-C (Fig. 1D).

(A.2) JAK/STAT signaling forms a gradient under the control of Upd and reaches the stationary state independently of the propagation of the proneural wave.

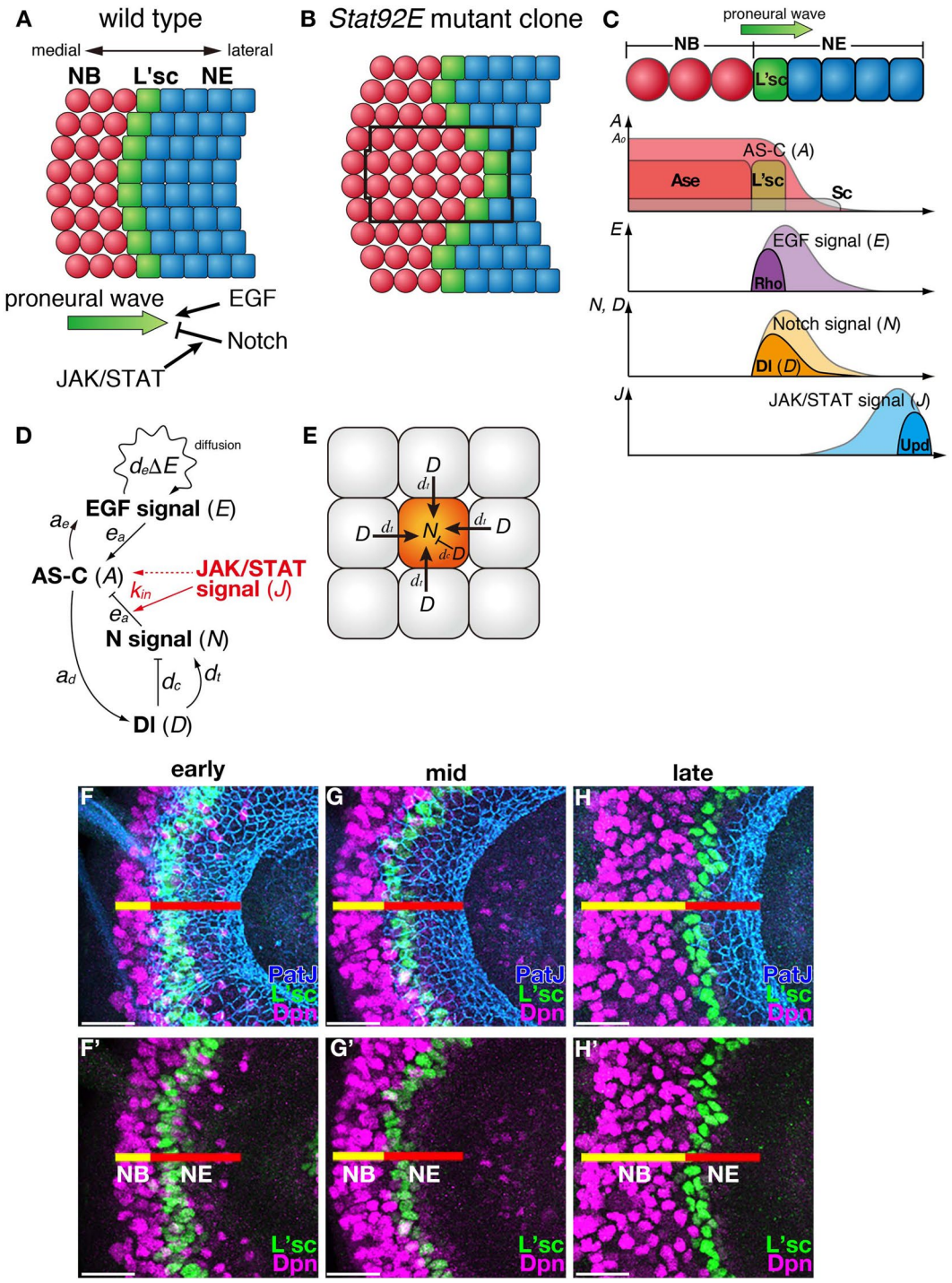

Figure 1. The proneural wave progresses unidirectionally during optic lobe development in *Drosophila*. (**A**) A schematic of the progression of the proneural wave. The proneural wave sweeps from medial to lateral. L'sc is transiently expressed in the differentiating NEs and defines the timing of the NE-to-NB differentiation. EGF positively regulates the progression of the wave, while Notch and JAK/STAT negatively regulate wave progression through increasing the expression of Notch target genes. (**B**) Summary of the loss-of-function phenotype of the *Stat92E* mutant clone. (**C**) Schema showing the spatial profile of each signaling activity. (**D**) Schema showing the gene regulatory network including AS-C, EGF, Notch, Dl, and JAK/STAT. (**E**) Lateral inhibition mechanism of Delta/Notch signaling. (**F**–**H'**) The progression of the proneural wave *in vivo*. Control third-instar larvae at (**F**) 114-126, (**G**) 126–138, (**H**) 138–150 hours after egg laying are shown. PatJ (blue, NE), L'sc (green, proneural wave), Deadpan (Dpn, magenta, NB) are shown. (**F'**, **G'**, and **H'**) L'sc (green) and Dpn (maenta) are shown. Scale bars, 20 μm.

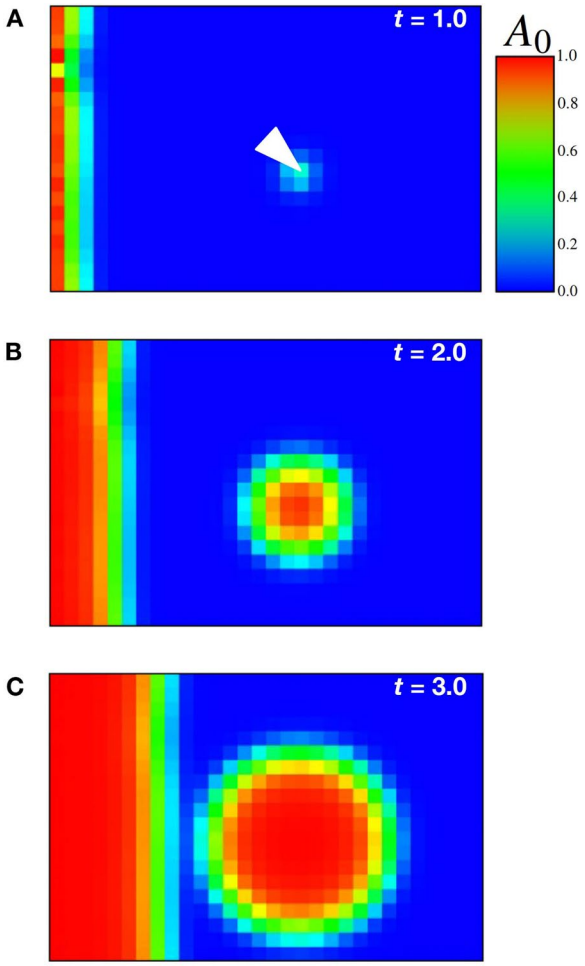

Figure 2. Minor perturbation of EGF signaling away from the wavefront causes spontaneous NB differentiation in Model 1. The small perturbation is imposed on E at the white arrow in the initial condition as shown in (**A**). The parameters are $d_e = 2.0$, $k_e = 1.0$, $a_e = 4.0$, $k_n = 3.0$, $d_t = 2.0$, $d_c = 0.1$, $k_d = 3.0$, $a_d = 4.0$, $e_a = 10.0$ and $A_0 = 1.0$. Panels (**A**–**C**) correspond to the profiles of A at $t = 1.0$, $t = 2.0$, and $t = 3.0$, respectively. The high and low expression levels of A are shown in red and blue as indicated in the color bar.

In Model 1, the effect of Notch corresponding to the *E(spl)mδ* and *E(spl)m7* is imposed inside the max function of the equation of A. This term regulates the trigger of the differentiation of A. Because JAK/STAT regulates these Notch target genes, we modified the fourth equation of Model 1 according to the assumption (A.1):

$$\frac{dA_{i,j}}{dt} = e_a(A_0 - A_{i,j})\max\{E_{i,j} - N_{i,j} - k_{in}J_\infty, 0\}, \tag{2}$$

where J is denoted by the JAK/STAT signaling at position x and time t and k_{in} is a positive constant for the regulation rate of JAK/STAT signaling for Notch target genes. Furthermore, from the assumption (A.2), as the JAK/STAT creates the gradient of its activation strongly in the lateral region and weakly in the medial region (Fig. S1), we impose J_∞ as a stationary state for the following reaction-diffusion model:

$$\begin{cases} \dfrac{\partial J}{\partial t} = d_i\Delta J - k_i J, \ (x, y) \in B, \ t > 0, \\ \dfrac{\partial J}{\partial y}(t, x, 0) = \dfrac{\partial J}{\partial y}(t, x, L_y) = 0, \ x \in [0, L_x], \\ \dfrac{\partial J}{\partial x}(t, 0, y) = 0, \ J(t, L_x, y) = J_0, \ y \in [0, L_y], \end{cases} \tag{3}$$

where d_i is a diffusion coefficient of the JAK/STAT signaling, k_i is a degradation rate, and J_0 is a positive constant corresponding to the JAK/STAT activation in the lateral region. From the first equation of eq. 3, the activity of JAK/STAT signaling is changed by the diffusion and the decay. We impose the zero flux boundary condition in the second formula similar to the eq. 1[13]. This indicates that the JAK/STAT activity is dependent on the distance

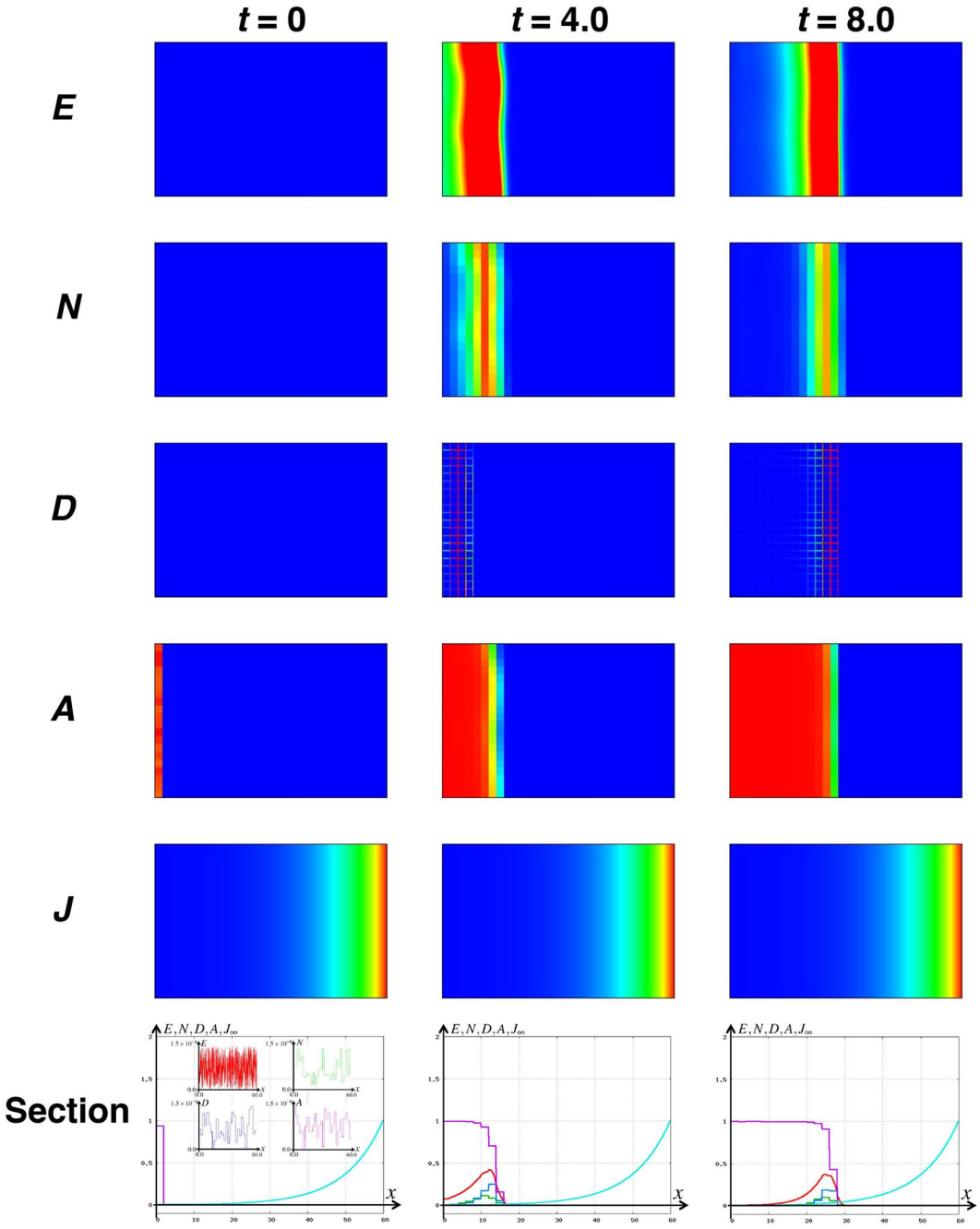

Figure 3. JAK/STAT signaling cancels the noise *in silico*. The result of the numerical simulation of Model 2 in the field B with the same parameters as in Fig. 2 and $k_{in} = 1.0$, $d_i = 1.0$, $k_i = 0.01$, $J_0 = 1.0$. The five upper figures show the profiles of the E, N, D, A, and J in the field B, and the lowest panels show the longitudinal section, where red, green, blue, magenta, and light blue curves correspond to the values of E, N, D, A, and J_∞ on $[0, L_x]$ and $y = L_y/2$. The columns from left to right show the profiles of $t = 0$, $t = 4.0$, and $t = 8.0$, respectively. The insets in the longitudinal section at $t = 0$ are enlarged views of E, N, D, and A at $t = 0$, and similar noise is added in each step in the numerical simulation.

from the ligand source and it shows the same value along with the y axis. In the third formula, we set activation of JAK/STAT as 0 at the medial side and J_0 at the lateral side, since JAK/STAT activation was not found in the medial most region in the optic lobe and the activation in the lateral side was always strong (Fig. S1). We designate the improved version from eq. 2 as Model 2. We next performed the numerical simulations with Model 2 in a two dimensional field, B (Fig. 3). Even in the presence of a small perturbation in the initial condition and in each step of all variables, the proneural wave propagates similarly to the noise-free condition because of the cancelation of the noise. This is explained from the perspective of mathematical modeling: In Model 2, the term inhibiting the differentiation of A is reproduced by the function $\max\{E_{i,j} - N_{i,j} - k_{in}J_\infty, 0\}$. If the concentration of $E_{i,j}$, which can promote the propagation of the proneural wave, is larger than that of $N + k_{in}J_\infty$, which inhibits the propagation

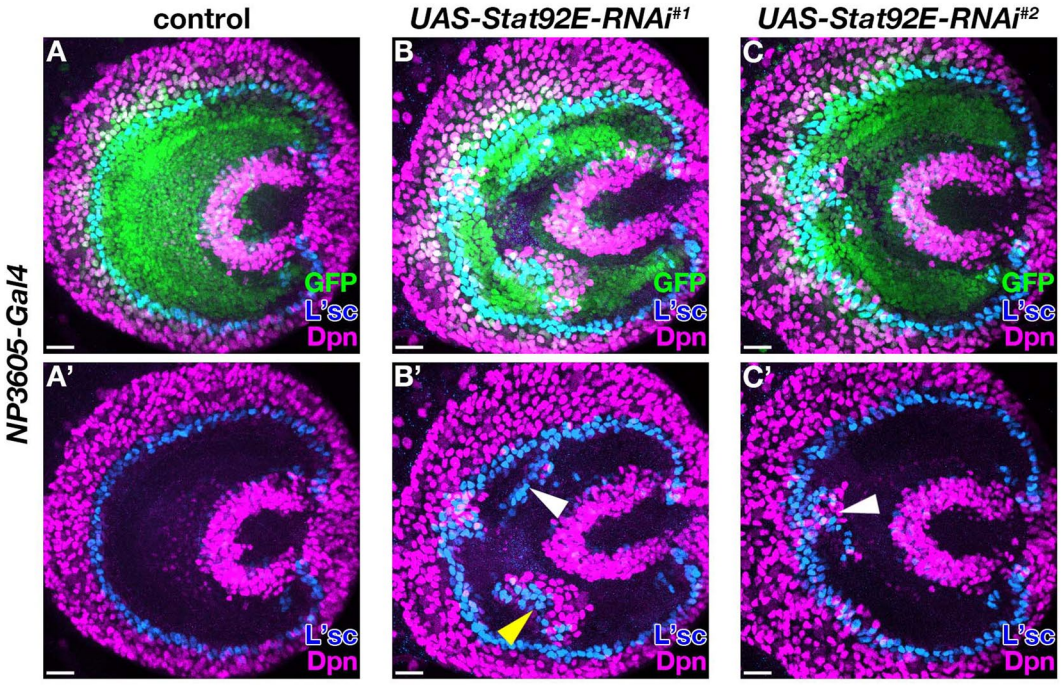

Figure 4. *Stat92E* blocks spontaneous neuroblast differentiation *in vivo*. (**A**–**C'**) Third-instar larval optic lobes for control (**A**), *UAS-Stat92E-RNAi*$^{\#1}$ (**B**), and *UAS-Stat92E-RNAi*$^{\#2}$ (**C**). *NP3605-Gal4 UAS-GFP.nls* (green), L'sc (blue) and Dpn (magenta) are shown. (**A'**–**C'**) L'sc and Dpn are shown. White arrowheads in (**B'**,**C'**) indicate ectopic L'sc and Dpn expression. The yellow arrowhead indicates ectopic L'sc expression medial to ectopic Dpn expression. Scale bars, 20 μm.

of the proneural wave in a cell, differentiation starts in that cell. On the other hand, *N* is not upregulated in the region distant from the wavefront[12]. Thus, stimulation of a small amount of noise to *E* eventually causes spontaneous NB differentiation. However, as the JAK/STAT signaling positively regulates Notch targets, the value inside the max function remains negative, even if a small perturbation is added into the concentration of *E* away from the wavefront. Thus, the spontaneous differentiation in the region distant from the wavefront is inhibited by the cancelation of the noise resulting from the function J_∞. As *E* is the only variable that increases the value inside the max function of *A*, total noise from other components can be integrated in *E*. Thus, we can determine that the noise can be canceled if the level of the noise of *E* is less than that of $k_{in}J_\infty$. The revised mathematical model still mimics *in vivo* situations and shows the capacity for noise resistance, suggesting that JAK/STAT signaling contributes to noise canceling during the progression of the proneural wave *in silico*.

In the current model, the noise resistance is less prominent when the position *x* is near the origin (Fig. 3). However, *in vivo*, the NE cells are dividing rapidly. Therefore, the undifferentiated region ahead of the wavefront is initially much smaller but is expanded as the wave propagates[8]. A future model that integrates the NE cell division will resolve this inconsistency.

JAK/STAT suppresses ectopic NB differentiation *in vivo*. Next, to confirm the possibility that JAK/STAT cancels spontaneous NB differentiation caused by biological noise *in vivo*, we reduced the JAK/STAT signaling activity by knocking down *Stat92E*. We induced *Stat92E* RNAi by using the *NP3605-Gal4* driver in the larval optic lobe NEs[12]. Two *Stat92E* RNAi lines targeting different regions of the *Stat92E* gene showed ectopic L'sc-positive differentiating cells and Deadpan (Dpn)-positive NBs in a stochastic manner (Fig. 4) (n = 16/18 for *UAS-Stat92E-RNAi*$^{\#1}$ and n = 18/44 for *UAS-Stat92E-RNAi*$^{\#2}$), suggesting that JAK/STAT does indeed cancel the biological noise. Additionally, the numerical simulation shows that the addition of noise away from the wavefront causes spontaneous NB differentiation in the opposite direction from that of the original proneural wave (Fig. 2). This numerical result was experimentally reproduced *in vivo*. Ectopic L'sc-expressing cells were sometimes found in the medial region, adjacent to ectopic Dpn-expressing cells, demonstrating that the ectopic NB differentiation wave progressed from the lateral to the medial direction in *STAT92E* RNAi samples (Fig. 4B', yellow arrowhead). To exclude the possibility that the effect of RNAi was not uniform and ectopic differentiation was caused where the JAK/STAT activity was particularly reduced by *Stat92E* RNAi, we examined the activation level of JAK/STAT signaling. 10×STAT-GFP, a JAK/STAT responsive reporter, was strongly expressed in the lamina and weakly in NEs in wild type optic lobes, as previously described (Fig. S1A)[8,15]. Expression of 10xSTAT-GFP was uniformly decreased in *Stat92E* RNAi samples (Fig. S1B and S1C) (n = 31/31 for *UAS-Stat92E-RNAi*$^{\#1}$ and n = 84/84 for *UAS-Stat92E-RNAi*$^{\#2}$). These experimental results suggest that JAK/STAT signaling is required *in vivo* for preventing spontaneous NB differentiation by suppressing the effects of noise.

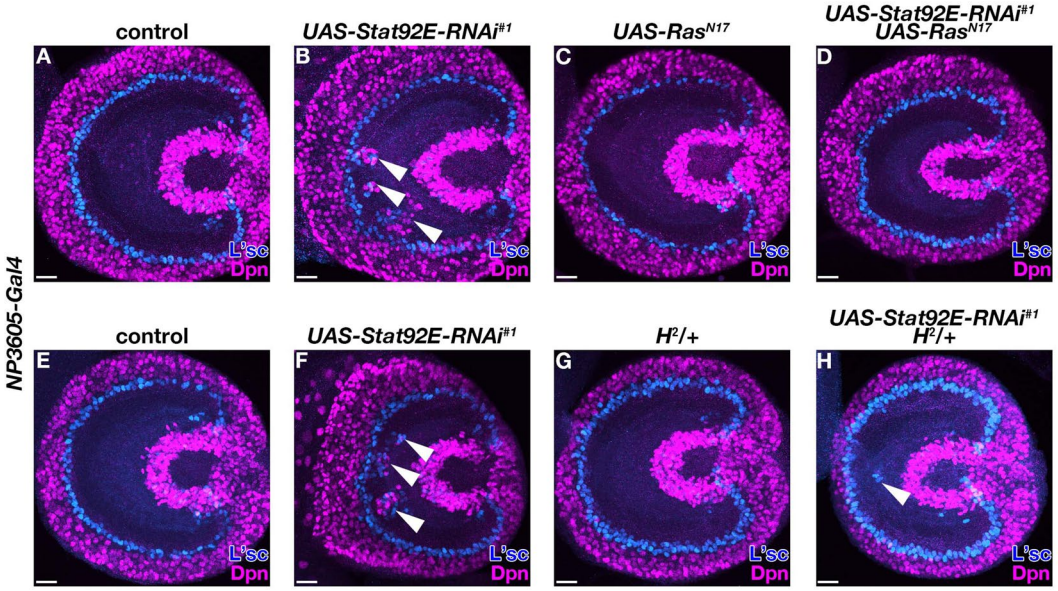

Figure 5. Noise canceling function of JAK/STAT is mediated by EGF and Notch signaling pathways. (**A**–**D**) Third-instar larval optic lobes for control (**A**), *UAS-Stat92E-RNAi*$^{\#1}$ (**B**), *UAS-Ras*^{N17} (**C**) and *UAS-Stat92E-RNAi*$^{\#1}$, *UAS-Ras*^{N17} (**D**). (**E**–**H**) Third-instar larval optic lobes for control (**E**), *UAS-Stat92E-RNAi*$^{\#1}$ (**F**), H^2 heterozygous mutant (**G**) and *UAS-Stat92E-RNAi*$^{\#1}$ in the H^2 heterozygous mutant background (**H**). *NP3605-Gal4* was used as a *Gal4* driver. L'sc (blue) and Dpn (magenta) are shown. White arrowheads in (**B**,**F**,**H**) indicate ectopic L'sc and/or Dpn expression. Scale bars, 20 μm.

Noise canceling function by JAK/STAT is mediated by EGF and Notch signaling pathways. In order to further dissect the noise canceling mechanism by JAK/STAT, we first asked whether activation of EGF signaling is required for ectopic NB differentiation under the *Stat92E* RNAi background. To reduce EGF activation, we expressed Ras^{N17}, a dominant negative form of Ras (Fig. 5A–D)[16]. Ras^{N17} expression in the control background did not show any phenotype (Fig. 5C) (n = 0/36). The phenotype of ectopic L'sc or Dpn expression by *Stat92E* RNAi (Fig. 5B) (n = 15/15) was suppressed by simultaneous expression of Ras^{N17} (Fig. 5D) (n = 0/58). This result suggests that EGF activation can be a source of noise which induces spontaneous NB differentiation under the decreased JAK/STAT activation condition.

We next examined the possibility that Notch signaling is involved in noise canceling. To test whether expression of *E(spl)mδ* and *E(spl)m7* is altered under the *Stat92E* RNAi condition, we checked expression pattern of E(spl)mδ-GFP and E(spl)m7-GFP. E(spl)mδ-GFP was expressed in cells in the lamina and in wavefront cells (Fig. S2A). E(spl)mδ-GFP expression in the lamina was disturbed when ectopic NB differentiation was induced by *Stat92E* RNAi (Fig. S2B) (n = 24/32). E(spl)m7-GFP was expressed in the lamina and NEs including wavefront cells (Fig. S2C). E(spl)m7-GFP was partially lost upon Stat92E knockdown (arrowhead in Fig. S2D) (n = 6/32). In both cases, GFP expression was only partially decreased, though *Stat92E* RNAi reduced the JAK/STAT activity uniformly (Fig. S1). Therefore, it is possible that JAK/STAT signaling regulates expression of these Notch target genes indirectly. To examine whether Notch signaling is involved in JAK/STAT-mediated noise canceling, we tested genetic interaction between the two signaling pathways (Fig. 5E–H). Hairless (H) acts as an antagonist to Notch signaling[17,18]. The ectopic NB differentiation phenotype by *Stat92E* RNAi (Fig. 5F) (n = 32/39) was partially suppressed in the H^2 heterozygous background (Fig. 5G,H) (n = 1/50 for 5 G and n = 13/45 for 5 H). This result suggests that Notch signaling acts downstream of JAK/STAT signaling to mediate the noise canceling function, though we cannot rule out the possibility that Notch signaling acts in parallel with JAK/STAT signaling (red arrows in Fig. 1D). Importantly, however, these two alternative possibilities are equivalent in our mathematical model (eq. 2).

Discussion

Although cellular events contain stochastic fluctuations, developmental processes progress precisely, and pattern formation is spatiotemporally organized, suggesting that there are regulatory mechanisms filtering the noise. In this report, we demonstrate that JAK/STAT signaling has a noise-canceling function during neural stem cell differentiation in the *Drosophila* optic lobe. From our mathematical model, any molecule which shows broad expression in NEs and negatively regulates EGF activation or expression of AS-C can cancel noise. However, we assume that JAK/STAT signaling plays the major role on noise canceling because JAK/STAT signaling is the only known factor which fits to the above assumptions and because the decrease of the JAK/STAT signal activation did show the ectopic neural stem cell differentiation phenotype[8]. JAK/STAT is involved in many developmental contexts and stem cell maintenance in both vertebrates and invertebrates[19–22]. Recent *in silico* experiments predict that Stat3 is involved in noise processing in mouse embryonic stem cells[23]. It is tempting to speculate that the

function of JAK/STAT in noise canceling is an evolutionally conserved fundamental mechanism to regulate the robustness of stem cell maintenance and differentiation.

Recently, a complementary strategy using both mathematical modeling and *in vivo* experiments has emerged as a powerful way to elucidate multiple types of biological noise within developmental systems[5,24]. By taking advantage of mathematical modeling, we can reveal how multicellular organisms cope with intrinsic and extrinsic noise to develop a robust system. Henceforth, by applying a combination of mathematical modeling and molecular genetics, we can solve biological questions that have previously been difficult to address.

Methods

Mathematical modeling. In the mathematical model, the calculation region is a two dimensional field $B = [0, L_x] \times [0, L_y]$ for positive constants $L_x, L_y > 0$ with the zero flux boundary condition. The field B is divided into square or hexagonal meshes in the numerical calculations, and each mesh is regarded as a cell with the indexes i and j corresponding to horizontal and vertical directions, respectively. Further, the variables without the indexes of i and j in the first equation of Model 1 indicate the variable for the whole region by combining each cell in the field B, and $E_{i,j}$ reproduces the averaging amount of E in the i, jth cell. Please refer the previous study[13] for the detailed mathematical settings.

Fly Genetics. Flies were grown at 25 °C, and *w* or *y w* flies were used as controls. *NP3605-Gal4 UAS-GFP.nls*, *UAS-Stat92E-RNAi*$^{\#1}$ (VDRC: 43866), *UAS-Stat92E-RNAi*$^{\#2}$ (VDRC: 106980), *UAS-Ras*^{N17} (BDSC: 4845), *10xSTAT-GFP* (BDSC: 26197), *E(spl)m7-GFP* (BDSC: 55839), *E(spl)mδ-GFP* (BDSC: 68191), and H^2 (BDSC: 517) flies were used.

Histology. Third-instar wandering larvae were dissected in PBS and fixed in 4% formaldehyde in PBS. Samples were washed three times after fixation with PBS containing 0.3% Triton X-100 and transferred to blocking solution (PBS containing 5% normal donkey serum and 0.3% Triton X-100). Specimens were incubated overnight at 4 °C with primary antibodies diluted in blocking solution. Primary antibodies were washed four times with PBS containing 0.3% Triton X-100 before the incubation overnight at 4 °C with secondary antibodies. Then, the samples were washed four times with PBS containing 0.3% Triton X-100. The primary antibodies used were as follows: rabbit anti-PatJ (1:1000), rat anti-Dpn (Abcam, 1:50), and guinea pig anti-L'sc (1:1200). The following secondary antibodies (Jackson) were used at 1:200 dilutions: FITC-conjugated donkey anti-rabbit, Cy3-conjugated donkey anti-rat, and Alexa Fluor 647-conjugated donkey anti-guinea pig. Specimens were mounted with VectaShield mounting media (Vector) and viewed on a Zeiss LSM880 confocal microscope. ZEN software (Zeiss) was used for preparing three-dimensional images.

Data availability. Data presented in this manuscript are tabulated in this published article and its Supplemental Information files.

References

1. Arias, A. M. & Hayward, P. Filtering transcriptional noise during development: concepts and mechanisms. *Nat. Rev. Genet.* **7**, 34–44 (2006).
2. Thattai, M. & van Oudenaarden, A. Intrinsic noise in gene regulatory networks. *Proc. Natl. Acad. Sci. USA* **98**, 8614–8619 (2001).
3. Becskei, A. & Serrano, L. Engineering stability in gene networks by autoregulation. *Nature* **405**, 590–593 (2000).
4. Raser, J. M. & O'Shea, E. K. Noise in gene expression: origins, consequences, and control. *Science* **309**, 2010–2013 (2005).
5. Horikawa, K., Ishimatsu, K., Yoshimoto, E., Kondo, S. & Takeda, H. Noise-resistant and synchronized oscillation of the segmentation clock. *Nature* **441**, 719–723 (2006).
6. Kepler, T. B. & Elston, T. C. Stochasticity in transcriptional regulation: origins, consequences, and mathematical representations. *Biophys. J.* **81**, 3116–3136 (2001).
7. Paulsson, J. Models of stochastic gene expression. *Phys. Life Rev.* **2**, 157–175 (2005).
8. Yasugi, T., Umetsu, D., Murakami, S., Sato, M. & Tabata, T. Drosophila optic lobe neuroblasts triggered by a wave of proneural gene expression that is negatively regulated by JAK/STAT. *Development* **135**, 1471–1480 (2008).
9. Sato, M., Suzuki, T. & Nakai, Y. Waves of differentiation in the fly visual system. *Dev. Biol.* **380**, 1–11 (2013).
10. Kawamori, H., Tai, M., Sato, M., Yasugi, T. & Tabata, T. Fat/Hippo pathway regulates the progress of neural differentiation signaling in the Drosophila optic lobe. *Dev. Growth Differ.* **53**, 653–667 (2011).
11. Reddy, B. V. V. G., Rauskolb, C. & Irvine, K. D. Influence of fat-hippo and notch signaling on the proliferation and differentiation of Drosophila optic neuroepithelia. *Development* **137**, 2397–2408 (2010).
12. Yasugi, T., Sugie, A., Umetsu, D. & Tabata, T. Coordinated sequential action of EGFR and Notch signaling pathways regulates proneural wave progression in the Drosophila optic lobe. *Development* **137**, 3193–3203 (2010).
13. Sato, M., Yasugi, T., Minami, Y., Miura, T. & Nagayama, M. Notch-mediated lateral inhibition regulates proneural wave propagation when combined with EGF-mediated reaction diffusion. *Proc. Natl. Acad. Sci. USA* **113**, E5153–5162 (2016).
14. Wang, H., Chen, X., He, T., Zhou, Y. & Luo, H. Evidence for tissue-specific Jak/STAT target genes in Drosophila optic lobe development. *Genetics* **195**, 1291–1306 (2013).
15. Bach, E. A. *et al.* GFP reporters detect the activation of the Drosophila JAK/STAT pathway *in vivo*. *Gene Expr Patterns* **7**, 323–331 (2007).
16. Lee, T., Feig, L. & Montell, D. J. Two distinct roles for Ras in a developmentally regulated cell migration. *Development* **122**, 409–418 (1996).
17. Bang, A. G., Bailey, A. M. & Posakony, J. W. Hairless promotes stable commitment to the sensory organ precursor cell fate by negatively regulating the activity of the Notch signaling pathway. *Dev. Biol.* **172**, 479–494 (1995).
18. Furriols, M. & Bray, S. Dissecting the mechanisms of suppressor of hairless function. *Dev. Biol.* **227**, 520–532 (2000).
19. Dorritie, K. A., Redner, R. L. & Johnson, D. E. STAT transcription factors in normal and cancer stem cells. *Adv. Biol. Regul.* **56**, 30–44 (2014).
20. Luo, H. & Dearolf, C. R. The JAK/STAT pathway and Drosophila development. *Bioessays* **23**, 1138–1147 (2001).
21. Amoyel, M. & Bach, E. A. Functions of the Drosophila JAK-STAT pathway: Lessons from stem cells. *JAKSTAT* **1**, 176–183 (2012).
22. Onishi, K. & Zandstra, P. W. LIF signaling in stem cells and development. *Development* **142**, 2230–2236 (2015).
23. Kontogeorgaki, S., Sanchez-Garcia, R. J., Ewing, R. M., Zygalakis, K. C. & MacArthur, B. D. Noise-processing by signaling networks. *Sci. Rep.* **7**, 532 (2017).
24. Li, C. J. *et al.* MicroRNA filters Hox temporal transcription noise to confer boundary formation in the spinal cord. *Nat. Commun.* **8**, 14685 (2017).

Acknowledgements

We thank Rie Takayama and members of Sato lab for supporting fly work, and H. J. Bellen, Bloomington Drosophila Stock Center (BDSC), Vienna *Drosophila* Stock Center, *Drosophila* Genetic Resource Center, Kyoto, for flies and antibodies. This work was supported by CREST (JPMJCR14D3 to M.S. and S.E.) from JST, Grant-in-Aid for Scientific Research on Innovative Areas (JP17H05739 to M.S., JP17H05761 to M.S., and JP18H05099 to T.Y.), Grant-in-Aid for Scientific Research (B) (JP17H03542 to M.S. and JP16H03949 to M.N.), and Grant-in-Aid for Young Scientists (B) (JP17K14228 to Y.T.) from MEXT, Takeda Science Foundation (to M.S.), and Cooperative Research of 'Network Joint Research Center for Materials and Devices' (to M.S. and M.N.).

Author Contributions

Y.T., M.N. and S.-I.E. designed and performed the modelling simulation. T.Y. and M.S. performed the genetic experiments and analyzed the data. Y.T., T.Y., M.N., M.S. and S.-I.E. wrote the manuscript.

Additional Information

Supplementary information accompanies this paper at https://doi.org/10.1038/s41598-018-30929-1.

Competing Interests: The authors declare no competing interests.

Publisher's note: Springer Nature remains neutral with regard to jurisdictional claims in published maps and institutional affiliations.

Open Access This article is licensed under a Creative Commons Attribution 4.0 International License, which permits use, sharing, adaptation, distribution and reproduction in any medium or format, as long as you give appropriate credit to the original author(s) and the source, provide a link to the Creative Commons license, and indicate if changes were made. The images or other third party material in this article are included in the article's Creative Commons license, unless indicated otherwise in a credit line to the material. If material is not included in the article's Creative Commons license and your intended use is not permitted by statutory regulation or exceeds the permitted use, you will need to obtain permission directly from the copyright holder. To view a copy of this license, visit http://creativecommons.org/licenses/by/4.0/.

© The Author(s) 2018